

**CHARACTERISTICS OF THE INTERFACIAL BONDING
BETWEEN NORMAL CONCRETE SUBSTRATE AND ULTRA
HIGH PERFORMANCE FIBER CONCRETE REPAIR MATERIAL**

by

BASSAM A. O. TAYEH

Thesis submitted in fulfillment of the requirements

for the degree of

Doctor of Philosophy

2013

**SIFAT IKATAN ANTARAMUKA ANTARA KONKRIT BIASA DAN
KONKRIT GENTIAN BERPRESTASI ULTRA TINGGI SEBAGAI
BAHAN BAIK PULIH**

oleh

BASSAM A. O. TAYEH

**Thesis yang diserahkan untuk
Memenuhi keperluan bagi
Doktor Falsafah**

2013

بِسْمِ اللَّهِ الرَّحْمَنِ الرَّحِيمِ

{ يَرْفَعِ اللَّهُ الَّذِينَ آمَنُوا مِنْكُمْ وَالَّذِينَ
أُوتُوا الْعِلْمَ دَرَجَاتٍ وَاللَّهُ بِمَا تَعْمَلُونَ خَبِيرٌ }

صدق الله العظيم

سورة المجادلة (11)

DEDICATION

To my loving parents who supported me at all the way; to my wife for her unlimited love, patience and encouragement ; to my children whose innocent energy was and still a source of inspiration; to all my brothers and sisters; to all of my friends and colleagues who stood beside me with great commitment; I dedicate this work, hoping that I made all of them proud.

Bassam A. O. Tayeh

ACKNOWLEDGEMENT

Alhamdulillah, first of all, I would like to express my grateful thanks to Allah SWT for his blessing and giving me the opportunity to accomplish my Ph.D study which was only a dream before. Then my grateful thanks also dedicated to my parents for all their pray and supporting me to finish my study.

I would like to express my grateful thanks to my supervisor Professor Dr. Badorul Hisham Abu Bakar for his guidance, advice, motivation and endless support, throughout this research. Also, I would like to thank my co-supervisor Associate Prof. Dr. Megat Azmi Megat Johari, for his continuous support, advice and constructive comments.

My special thanks and appreciation for Professor Dr. Mani Maran Ratnam, from School of Mechanical Engineering, USM and Dr. Yen Lei Voo, from Dura Technology Sdn. Bhd., Perak, Malaysia, for their advice and scientific comments.

I sincerely would like to thank all the academic staff, official staff and my colleagues in the School of Civil Engineering (USM) for their help and moral support. Thanks are also extended for the technicians in the concrete laboratory especially Mr. Shahril Izham bin Md. Noor; Mr. Mohd Fauzi bin Zulkfle; Mr. Abdullah bin Md Nanyan; Mr. Mad Fadzil Ali and Mr. Mohd Taib bin Yaacob, for their help.

I would like to express my great thanks to my University Sains Malaysia (USM) which I always feel belonging to, for the financial support for this research. Special thanks for School of Material and Mineral Resources Engineering (USM), School of Mechanical Engineering (USM), for using their labs to perform some tests.

TABLE OF CONTENTS

	Page
DEDICATION	I
ACKNOWLEDGEMENT	II
TABLE OF CONTENTS	III
LIST OF TABLES	X
LIST OF FIGURES	XII
LIST OF ABBREVIATIONS	XX
LIST OF SYMBOLS	XXII
ABSTRAK	XXIV
ABSTRACT	XXVI
CHAPTER 1: INTRODUCTION	
1.1 Background and Rationale	1
1.2 Problem Statement	3
1.3 Research Objectives	7
1.4 Scope	7
1.5 Thesis Outline	9
CHAPTER 2 : LITERATURE REVIEW	
2.1 Introduction	10
2.2 Ultra high performance fiber concrete (definitions, contents, properties and applications)	10
2.2.1 Definitions of Ultra high performance fiber concrete	12
2.2.2 Ultra-high performance fiber concrete components	13

2.2.2.1	Typical Mix of Ultra high performance fiber concrete	13
2.2.2.2	Ultra-high performance fiber concrete constituents	15
2.2.3	Properties of Ultra-high performance fiber concrete	21
2.2.3.1	Tensile behavior	21
2.2.3.2	Flexural strength	22
2.2.3.3	Durability	23
2.2.3.4	Curing of UHPFC	24
2.2.3.5	Shrinkage	25
2.2.3.6	Chloride penetration	27
2.2.3.7	Comparison between concrete types	28
2.2.4	Applications of UHPFC	31
2.2.4.1	Structural applications	31
2.2.4.2	Architectural applications	40
2.3	Use of UHPFC in rehabilitation	44
2.3.1	Concrete structures need rehabilitations	44
2.3.2	Potential of UHPFC as a repair material	45
2.3.3	Applications of UHPFC in rehabilitation	49
2.3.3.1	Bridge over the river La Morge, Switzerland	50
2.3.3.2	Log Čezoški Bridge, Slovenia	51
2.3.3.3	Valabres Bridge, France	52
2.4	Bonding strength between repair material and concrete substrate	54
2.4.1	Introduction	54
2.4.2	Evaluation of the bonding strength between repair material and concrete substrate	55
2.4.2.1	Tensile tests	57

2.4.2.2	Slant shear bond strength	60
2.4.3	Interfacial transition zone in repair system	62
2.4.3.1	Effect of roughness of the substrate surface on the bond strength	63
2.4.3.2	Effect of substrate surface moistures on bond strength	67
CHAPTER 3: RESEARCH METHODOLOGY		
3.1	Introduction	72
3.2	Materials for research	74
3.2.1	Normal concrete substrate	74
3.2.1.1	Mix proportions and mixing procedures	74
3.2.2	UHPFC as a repair material	77
3.2.2.1	UHPC mixing proportions	77
3.2.2.2	Mixing procedures of UHPFC	79
3.2.2.3	Flowbility of UHPFC	83
3.2.2.4	Setting time	84
3.2.2.5	Curing of UHPFC	85
3.3	Surface roughness of NC substrate	86
3.3.1	NC substrate surface preparation	86
3.3.1.1	Without surface preparation (AC)	87
3.3.1.2	Sand blasted surface (SB)	88
3.3.1.3	Wire-brushed (WB)	89
3.3.1.4	Drilled holes (DH)	90
3.3.1.5	Grooves (GR) 10 mm width and 5 mm depth	92
3.3.2	Quantification of the NC substrate surface roughening parameters	93

3.3.2.1	Roughness parameters	94
3.4	Engineering properties of NC, UHPFC and composite UHPFC/NC substrate	97
3.4.1	Compression testing	97
3.4.2	Modulus of elasticity	99
3.4.3	Slant shear test	102
3.4.3.1	NC and UHPFC specimens preparation	102
3.4.3.2	Composite UHPFC/NC substrate specimens preparation	104
3.4.4	Splitting cylinder tensile test (ASTM C496)	109
3.4.4.1	NC substrate and UHPFC specimens preparation	110
3.4.4.2	Composite UHPFC/NC substrate specimens preparation	111
3.4.5	Pull off test	114
3.4.5.1	Composite UHPFC/NC substrate specimens preparation	114
3.4.6	Third point loading beam test method for compatibility of repair materials (Flexural strength)	120
3.4.6.1	NC and UHPFC specimens preparation	121
3.4.6.2	Composite UHPFC/NC substrate specimens preparation	123
3.5	Permeability tests	125
3.5.1	Rapid chloride permeability test (ASTM C1202-94)	126
3.5.1.1	NC substrate and UHPFC	127
3.5.1.2	Composite UHPFC/NC substrate	128
3.5.2	Chloride penetration depth test	131
3.5.3	Gas permeability	131
3.5.3.1	NC substrate and UHPFC	133
3.5.3.2	Composite UHPFC/NC substrate	134

3.5.4	Water permeability test	136
3.5.5	Porosity and water absorption tests	138
3.5.6	Microstructure of the transition zone between the NC substrate and UHPFC	141
CHAPTER 4: RESULTS AND DISCUSSION		
4.1	Introduction	143
4.2	The mechanical properties of NC substrate and UHPFC	143
4.2.1	Compressive strength	144
4.2.1.1	Compressive strength of cubes	144
4.2.1.2	Compressive strength of prism	145
4.2.2	Modulus of elasticity	146
4.2.3	Splitting tensile strength	147
4.2.4	Flexural strength	147
4.3	Mechanical properties of the composite UHPFC/NC substrate	149
4.3.1	Slant shear test	149
4.3.1.1	Failure modes	149
4.3.1.2	Effect of substrate surface preparation	155
4.3.1.3	The behavior of slant shear bond strength with time	158
4.3.1.4	Effect of the substrate moistening on the slant shear bond strength	163
4.3.2	Splitting tensile strength test	165
4.3.2.1	Failure modes	165
4.3.2.2	Effect of substrate surface preparation	170
4.3.2.3	The behavior of the splitting cylinder tensile bond strength with time	173

4.3.2.4	Effect of substrate moistening on the splitting tensile bond strength	177
4.3.3	Pull-off test	180
4.3.3.1	Failure modes	180
4.3.3.2	Effect of substrate surface preparation	186
4.3.3.3	The behavior of the pull-off bond strength with time	187
4.3.3.4	The effect of substrate moistening on the pull-off bond strength	188
4.3.4	Flexural test	189
4.3.4.1	Failure Modes	189
4.3.4.2	Effect of substrate surface preparation	193
4.3.4.3	Development of flexural strength with time	193
4.3.4.4	The effect of the substrate moistening on the flexural test of the composite prism of UHPFC/NC substrate	194
4.4	NC substrate surface roughness	194
4.4.1	Roughness parameters	194
4.4.2	Correlation between substrate roughness parameters and bond strength	200
4.5	Microstructure of interfacial transition zone between NC substrate and UHPFC	206
4.6	The permeability properties of the NC substrate, UHPFC and composite UHPFC/NC substrate	213
4.6.1	Rapid chloride permeability test	213
4.6.2	Gas permeability	218
4.6.3	Water permeability	220
4.6.4	Porosity	225

4.7 General discussion	227
------------------------	-----

CHAPTER 5: CONCLUSIONS and RECOMMENDATIONS

5.1 General	229
5.2 The mechanical properties of the bonded UHPFC/NC substrate	230
5.3 The permeability properties of the bonded UHPFC/NC substrate	231
5.4 NC substrate roughness and its influence on the bonding with UHPFC	232
5.5 Interface microstructure of the bonded UHPFC/NC substrate	233
5.6 Recommendations for future research	234

REFERENCES	236
-------------------	-----

APPENDICES

APPENDIX A

APPENDIX B

LIST OF AWARDS AND PUBLICATIONS

LIST OF TABLES

		Page
Table 2.1	Range of UHPFC mix components	14
Table 2.2	Chloride ion permeability for different curing regime of UHPFC specimens	28
Table 2.3	Material characteristics of UHPdC compared with NC and HPC	30
Table 3.1	Chemical compositions of Ordinary Portland Cement (OPC)	75
Table 3.2	NC substrate mix proportions	76
Table 3.3	Chemical compositions of silica fume	78
Table 3.4	UHPFC mix proportions	79
Table 3.5	UHPFC mixing procedures	81
Table 3.6	Flow domain classifications of freshly mixed UHPFC	84
Table 3.7	The different specimens used for slant shear test	109
Table 3.8	Summary of pull off test specimens	119
Table 3.9	Summary of flexural test specimens	125
Table 3.10	Chloride ion penetrability based on charge passed	127
Table 4.1	Compressive strength of UHPFC	144
Table 4.2	Average compressive strength of NC substrate and UHPFC prism sample (100 x 100 x 300 mm)	146
Table 4.3	Modulus of elasticity of NC substrate and UHPFC	147
Table 4.4	Average splitting tensile strength of NC substrate and UHPFC	147
Table 4.5	Average flexural strength of NC substrate and UHPFC	148

Table 4.6	Slant shear strength and failure modes of composite UHPFC/NC substrate specimens, (10 min. moistening)	153
Table 4.7	Slant shear strength and failure modes of composite UHPFC/NC substrate specimens, (24h moistening)	153
Table 4.8	The relative increase in slant shear strength for different types of substrate surface roughness at different ages (10 min. moistening)	156
Table 4.9	The relative increase in slant shear strength for different types of substrate surface roughness (24h. moistening)	156
Table 4.10	Acceptable bond strength range (ACI Concrete Repair Guide)	159
Table 4.11	Splitting tensile strength and failure modes of composite UHPFC/NC substrate specimens, (10 min. moistening)	166
Table 4.12	Splitting tensile strength and failure modes of composite UHPFC/NC substrate specimens, (24h. moistening)	167
Table 4.13	The relative increase in splitting strength for different types of surface roughness, (10 min moistening)	171
Table 4.14	The relative increase in splitting strength for different types of surface roughness, (24 h moistening)	172
Table 4.15	Quantitative bond quality in term of bond strength	176
Table 4.16	Pull off bond strength and failure mode (10 minutes moistening)	183
Table 4.17	Pull off bond strength and failure mode (24 hours moistening)	184
Table 4.18	Flexural strength and failure modes of composite UHPFC/NC substrate specimens, (10 min moistening)	190
Table 4.19	Flexural strength and failure modes of composite UHPFC/NC substrate specimens, (24 h moistening)	191
Table 4.20	Roughness parameters for the different substrate surfaces	200

LIST OF FIGURES

		Page
Figure 2.1	Classification of FRC	12
Figure 2.2	Steel fiber	20
Figure 2.3	Relative density versus water content	20
Figure 2.4	Uniaxial tensile behavior: comparing UHPFC, conventional SFRC, and conventional concrete	21
Figure 2.5	Flexural strength versus midspan displacement	22
Figure 2.6	Durability of UHPC and HPC versus NC (lowest values identify the most favorable material)	23
Figure 2.7	Conditions of standard heat curing	24
Figure 2.8	Porosity of heat-treated and untreated UHPFC	25
Figure 2.9	Long-term autogenous shrinkage at 20 °C as a function of time	26
Figure 2.10	Effect of fibers on autogenous shrinkage at 20 °C as a function of time	27
Figure 2.11	Sherbrooke Pedestrian Bridge Quebec, Canada	32
Figure 2.12	Footbridge of Peace in Seoul, South Korea	33
Figure 2.13	The Sakata-Mirai footbridge in Japan	33
Figure 2.14	Bourg les Valence Road Bridge, France	34
Figure 2.15	Shepherd Creek Road Bridge in New South Wales, Australia	35
Figure 2.16	Mars Hill Bridge in Wapello County, Iowa	36
Figure 2.17	Gaertnerplatz Bridge in Kassel: (a) under construction and (b) in use	37

Figure 2.18	View of Haneda Airport Runway D	38
Figure 2.19	Longitudinal connections cast between deck-bulb-tee girders on Route 31 Bridge in Lyons, New York	39
Figure 2.20	Kampung Linsum Bridge, Rantau, Negeri Sembilan	40
Figure 2.21	Martel Tree sculpture made of UHPFC	41
Figure 2.22	Shawnessy LRT station with UHPFC canopies	42
Figure 2.23	Overview of the cover of Millau Toll	43
Figure 2.24	Wilson Hall during the construction	44
Figure 2.25	Cross section of the bridge (a) before and (b) after rehabilitation (dimensions in cm)	51
Figure 2.26	Cross section of bridge rehabilitated with UHPFC	52
Figure 2.27	Repair and protection of foundations and supports of Valabres bridge	53
Figure 2.28	Direct tension test	56
Figure 2.29	Indirect tension test	56
Figure 2.30	Pull-Off test	56
Figure 2.31	Direct shear test	56
Figure 2.32	Slant shear test	56
Figure 2.33	Splitting tensile strength test	57
Figure 2.34	Pull-Off test	59
Figure 2.35	Flexural test (a) specimen arrangement; (b) third point loading beam test.	59
Figure 2.36	Substrate and composite section for slant shear bond strength test	61
Figure 2.37	Slant shear test	61

Figure 2.38	Measuring the substrate texture	66
Figure 3.1	Flow chart depicting the methodology used in this chapter.	73
Figure 3.2	Mixing procedures of UHPFC	82
Figure 3.3	Impact table measurement of UHPC's Flow	84
Figure 3.4	Measuring the initial and final setting time of the UHPFC	85
Figure 3.5	Conditions of standard heat curing	86
Figure 3.6	Cleaning of the as-cast surface	88
Figure 3.7	Sand-basting machine	89
Figure 3.8	Application of wire-brushed on NC substrate	90
Figure 3.9	Application of drill-holes on NC substrate	91
Figure 3.10	Application of grooves on NC substrate	92
Figure 3.11	An optical 3D surface metrology device	93
Figure 3.12	Average roughness R_a	95
Figure 3.13	Mean peak-to-valley height, R_z	96
Figure 3.14	A compression machine with maximum capacity of 3000 kN	98
Figure 3.15	Compressive strength test for (a) NC substrate and (b) UHPFC	99
Figure 3.16	(a) Grinding the cylinder surface and (b) leveling the surface of samples	100
Figure 3.17	(a) extracting UHPFC cylinders (b) performing the compression test.	101
Figure 3.18	A Shimadzu UH-F 1000 kN Universal Testing Machine used for determining modulus of elasticity	101

Figure 3.19	Compression test set-up for (a) NC specimens and (b) UHPFC specimens	104
Figure 3.20	The geometry of half NC substrate specimen for slant shear (dimensions in mm)	105
Figure 3.21	Slant shear test specimens with five different surface textures.	106
Figure 3.22	(a) NC substrate prior to overlaying of UHPFC and (b) slant shear test set-up for the composite specimen	107
Figure 3.23	Steam curing of the composite UHPFC/ NC substrate samples	108
Figure 3.24	Splitting cylinder tensile test (a) NC specimens and (b) UHPFC specimens.	111
Figure 3.25	(a) The cylinder mould with a steel separator (b) NC substrate halves of splitting tensile test specimens with the different surface textures	112
Figure 3.26	(a) NC substrate prior to overlaying of UHPFC and (b) splitting tensile test set-up for the composite specimen	113
Figure 3.27	NC substrate specimens with different surface textures for pull off test: a. As-cast (AC) b. Sand-blasted (SB) and c. Wire-brushed (WB)	116
Figure 3.28	(a) Composite UHPFC/NC substrate (b) Pull off test set-up for the composite specimen	117
Figure 3.29	Schematic diagram of pull-off testing and specimen prepared	118
Figure 3.30	Diagrammatic view of a suitable apparatus for flexural test of concrete by third-point loading method	120
Figure 3.31	(a) AUTOGRAPH AG-X, Universal Testing Machine, (b) Flexural strength test set-up for NC specimens and (c) Flexural strength test set-up for UHPFC specimens.	122
Figure 3.32	NC substrate with different surface treatment, for flexural test	123

Figure 3.33	(a) NC substrate prior to overlaying of UHPFC and (b) the third-point loading beam test set-up for the composite specimen	124
Figure 3.34	Rapid chloride permeability test	128
Figure 3.35	a. Composite (UHPFC/NC substrate) cylinder. b. Composite (UHPFC/NC substrate) HH slice for RCPT test	129
Figure 3.36	a. Composite (UHPFC/NC substrate) slab. b. Composite (UHPFC/NC substrate) OV slice for RCPT test	130
Figure 3.37	Experimental setup for gas permeability test	133
Figure 3.38	NC and UHPFC specimens for gas permeability	134
Figure 3.39	Composite UHPFC/NC substrate, (a) composite prisms; (b) HH composite specimens	135
Figure 3.40	Composite (UHPFC/NC substrate) OV slice for gas permeability test	136
Figure 3.41	A vacuum desiccators, used to porosity test	140
Figure 3.42	Scanning Electron Microscopy	141
Figure 3.43	Core sample extracted from the interface between NC substrate and UHPFC for SEM test	142
Figure 4.1	Compression test for prism sample (100 x 100 x 300 mm)	146
Figure 4.2	Flexural test failure pattern (a) NC substrate and (b) UHPFC	149
Figure 4.3	Failure modes of slant shear strength test: (a) Failure mode A= Interface failure, (b) Failure mode B = Interface failure and substrate cracks, (c) Failure mode C = Interface failure and substrate fracture and (d) Failure mode D = Substratum failure with good interface	152
Figure 4.4	The average relative increase in slant shear strength for the different types of substrate surface roughness at all ages (10 min. moistening)	157

Figure 4.5	The average relative increase in slant shear strength for the different types of substrate surface roughness at all ages (24h. moistening)	157
Figure 4.6	Average slant shear strength for the different type of substrate surface at different ages (10 min. moistening)	162
Figure 4.7	Average slant shear strength for the different type of substrate surface at different ages. (24 h moistening)	163
Figure 4.8	Failure modes of splitting tensile strength test: (a) Failure mode A = interfacial failure; (b) Failure mode B = interfacial failure with partial substrate failure and (c) Failure mode C = substratum failure	168
Figure 4.9	Average relative increase in splitting tensile strength for different types of substrate surface roughness at all ages (10 min moistening)	172
Figure 4.10	Average relative increase in splitting tensile strength for different types of substrate surface roughness at all ages (24h. moistening)	173
Figure 4.11	Average splitting tensile strength for different types of substrate surface at different ages (10 min. moistening)	175
Figure 4.12	Average splitting tensile strength for different types of substrate surface at different ages (24 h moistening).	176
Figure 4.13	Correlation between slant shear test and splitting tensile test results (10 min. moistening) at: (a) 3 days; (b) 7 days; (c) 14 days; (d) 28 days; (e) 90 days and (f) 180 days	178
Figure 4.14	Correlation between slant shear test and splitting tensile test results (24 h moistening) at: (a) 3 days; (b) 7 days; (c) 14 days; (d) 28 days; (e) 90 days and (f) 180 days	179
Figure 4.15	Substrate surface prepared with: (a) as-cast, (b) wire-brushed and (c) sand-blasted	181
Figure 4.16	(a) Composite UHPFC/NC substrate, (b) Pull off test set-up for the composite specimen, (c) Failure through the NC substrate	182

Figure 4.17	Expected failure modes of specimens of pull off test	187
Figure 4.18	Flexural failure of composite UHPFC/NC substrate, (a) as-cast surface, (b) wire-brushed surface and (c) sand-blasted surface.	192
Figure 4.19	The roughness profiles for different surface treatments of NC substrate, (a) as-cast surface, (b) wire-brushed surface, (c) sand-blasted surface, (d) drill-holes surface and (e) grooved surface	198
Figure 4.20	Correlation between average roughness profile (Ra) and slant shear strength results for 10 min moistening, at different ages	202
Figure 4.21	Correlation between average roughness profile (Ra) and slant shear strength results for 24h moistening, at different ages	203
Figure 4.22	Correlation between average roughness profile (Ra) and the splitting tensile strength results for 10 min moistening, at different ages	204
Figure 4.23	Correlation between average roughness profile (Ra) and the splitting tensile strength results for 24h min moistening, at different ages	205
Figure 4.24	SEM/EDS of the interfacial transition zone between UHPFC and as-cast NC substrate for pull-off test at 28 days	209
Figure 4.25	SEM/EDS of the interfacial transition zone between UHPFC and wire-brushed NC substrate for pull-off test at 28 days	211
Figure 4.26	SEM/EDS of the interfacial transition zone between UHPFC and sand-blasted NC substrate for pull-off test at 28 days	212
Figure 4.27	SEM micrograph of the transition zone between NC substrate and UHPFC overlay for slant shear test at 28 days	214
Figure 4.28	Comparison of the rapid chloride permeability test results between NC substrate, UHPFC and composite UHPFC/NC substrate (HH, 10 min moistening)	215
Figure 4.29	Comparison of the rapid chloride permeability test results between NC substrate, UHPFC and composite UHPFC/NC substrate (HH, 24 h moistening)	215

Figure 4.30	Comparison of the rapid chloride permeability test results between NC substrate, UHPFC and composite UHPFC/NC substrate (OV, 10 min moistening)	216
Figure 4.31	Comparison of the rapid chloride permeability test results between NC substrate, UHPFC and composite UHPFC/NC substrate (OV, 24 h moistening)	216
Figure 4.32	Specimens of RCPT test, a- NC substrate specimens, b- UHPFC specimens and c- composite UHPFC/NC substrate specimens.	217
Figure 4.33	Comparison of the gas permeability test results between NC substrate, UHPFC and composite UHPFC/NC substrate (HH, 10 min moistening)	219
Figure 4.34	Comparison of the gas permeability test results between NC substrate, UHPFC and composite UHPFC/NC substrate (HH, 24 h moistening)	219
Figure 4.35	Comparison of the gas permeability test results between NC substrate, UHPFC and composite UHPFC/NC substrate (OV, 10 min and 24 h moistening)	220
Figure 4.36	Comparison of the water permeability test results between NC substrate, UHPFC and composite UHPFC/NC substrate (HH, 10 min moistening)	222
Figure 4.37	Comparison of the water permeability test results between NC substrate, UHPFC and composite UHPFC/NC substrate (HH, 24 h moistening)	222
Figure 4.38	Comparison of the water permeability test results between NC substrate, UHPFC and composite UHPFC/NC substrate (OV, 10 min moistening)	223
Figure 4.39	Specimens of water permeability test, a- NC substrate specimens, b- composite UHPFC/NC substrate specimens	224
Figure 4.40	Comparison of the porosity test results between NC substrate, UHPFC and composite UHPFC/NC substrate (HH, 10 min moistening)	226
Figure 4.41	Comparison of the porosity test results between NC substrate, UHPFC and composite UHPFC/NC substrate (HH, 24 h moistening)	226

LIST OF ABBREVIATIONS

AC	as cast
ACI	American Concrete Institute
ADF	amplitude distribution function
ASTM	American Society for Testing and Materials
BS EN	British European Standards Specifications
COV	coefficient of variation
C-S-H	calcium silicate hydrate
DEF	delayed ettringite formation
DR	drilled holes
GDP	gross domestic product
GR	grooved
HH	half NC and half UHPFC
HPC	High performance concrete
ISO	International Standard Organization
NC	normal concrete
OPC	Ordinary Portland Cement
OV	overlay
RC	reinforced concrete
RCPT	rapid chloride permeability test
RPC	reactive powder concrete

SB	sand blasted
SEM	scanning electron microscope
SFRC	steel fiber reinforcement concrete
SiO ₂	silicon dioxide
TCP	total charge passed
UHPFC	ultra high performance fiber concrete
V	DC voltage
WB	wire brushed
w/b	water/binder ratio
w/c	water/cement ration
WPT	water permeability test
XRD	x-ray diffraction

LIST OF SYMBOLS

A	cross-sectional area of cored sample
A_f	bonded area of the pull-off surface
A_L	bonded area of the slant shear surface
A_T	bonded area in splitting cylinder tensile test
d	water penetration depth
d_f	diameter of steel fiber
f_{cc}	cube compressive strength
f_{sp}	splitting cylinder tensile strength
F_T	tensile (pull-off) force at failure
h	applied pressure
K_w	coefficient of water permeability
L_f	length of steel fiber
l_m	length of roughness profile
m	gain in mass
p_{in}	inlet pressure
p_{out}	outlet pressure
P	maximum force
Q	gas flow
R_a	average roughness
R_q	root-mean-square average roughness
R_t	total roughness

R_p	highest peak in the roughness profile over the evaluation length
R_v	deepest valley in the roughness profile over the evaluation length
R_z	mean peak-to-valley height of roughness profile
R_{sk}	Skewness, is one such parameter that describes the shape of the ADF
R_{ku}	Kurtosis, is a parameter to identify the uniformity of ADF
S	slant shear strength
S_{po}	pull-off bond strength
t	time under pressure
T	splitting cylinder tensile strength
w_d	mass of oven dry sample
w_{ssd}	mass of sample in saturated and surface dry condition
w_{ssw}	mass of sample in water
μ	coefficient of viscosity of the gas
ρ	density of water
v	porosity of concrete

SIFAT IKATAN ANTARAMUKA ANTARA KONKRIT BIASA DAN KONKRIT GENTIAN BERPRESTASI ULTRA TINGGI SEBAGAI BAHAN BAIK PULIH

ABSTRAK

Sebagai satu peraturan kebiasaan, ikatan antaramuka struktur konkrit lama dengan lapisan baru bahan baik pulih merupakan salah satu faktor penting untuk memastikan struktur berfungsi dengan baik, selamat serta tahan lasak. Oleh itu, untuk meningkatkan rintangan terhadap penetrasi bahan-bahan yang merosakkan, satu ikatan yang baik dan efektif di perlukan antara permukaan struktur konkrit berkenaan. Objektif kajian ini adalah untuk mengkaji sifat-sifat mekanikal, ciri-ciri ketelapan jangka masa pendek dan panjang antara ikatan konkrit biasa (NC) dengan lapisan konkrit gentian berprestasi ultra tinggi (UHPFC) sebagai bahan baik pulih. Untuk menguji sifat-sifat mekanikal dalam ikatan, ujian lereng ricih (*slant shear*), ujian ketegangan (*splitting tensile*), Pull off test dan ujian lenturan (*flexural test*) dijalankan bagi menentukan pengaruh kepelbagaian kekasaran permukaan serta kesan kelembapan terhadap permukaan tersebut. Selain itu, kajian mengenai ciri-ciri ketelapan telah diuji dengan menggunakan kaedah ketelapan klorida (*rapid chloride permeability*), ujian ketelapan gas dan air serta ujian keporosan. Dalam kajian ini terdapat lima (5) jenis tekstur permukaan yang telah digunakan iaitu tuangan (AC) (tanpa penyediaan permukaan), letupan pasir (SB), gosokan dawai (WB), mengerudi lubang (DH) dan berlurah (GR). Kekasaran bagi setiap jenis tekstur permukaan ditentukan dengan menggunakan peranti metrologi 3 dimensi (*Alicona Infinite Focus*). Selain itu, mikrostruktur zon peralihan antara permukaan juga dikaji dengan menggunakan mikroskop elektron pengimbasan (*electron microscopy*) dan tenaga spektroskopi sinar X (*energy dispersive X-ray spectroscopy* (SEM/EDS)). Keputusan bagi jangka masa pendek dan panjang menunjukkan bahawa

lapisan baru (UHPFC) mencapai tahap kekuatan ikatan yang tinggi dan terikat dengan memuaskan dengan konkrit biasa. Ujian lenturan dan ujian tarik keluar (*pull off test*) menunjukkan bahawa semua kegagalan berlaku pada substratum tanpa mengira kekasaran pada permukaan substratum tersebut. Keputusan ujian lereng ricih (*slant shear*) dan ujian ketegangan (*splitting tensile*) juga menunjukkan bahawa kegagalan berlaku pada substratum. Gabungan bahan UHPFC/NC yang mempunyai permukaan letupan pasir (SB) berkelakuan menghampiri struktur monolitik apabila diuji menggunakan kaedah ujian ketegangan dan ujian lereng ricih. Nilai hubungan kait yang sangat baik ($R^2 > 80\%$) bagi setiap ujikaji telah diperolehi antara parameter kekasaran substratum, silinder koyak tegang (*splitting cylinder tensile*) dan lereng ricih (*slant shear*). Hasil ujian ketelapan telah menunjukkan ikatan antara permukaan sangat baik. SEM / EDS membuktikan bahawa penggunaan UHPFC sebagai bahan pembaik pulih secara kimia, fizikal dan mekanikal mampu meningkatkan lagi penambahbaikan zon peralihan antara permukaan menjadi lebih kukuh, padat, seragam, serta tahan lasak.

CHARACTERISTICS OF THE INTERFACIAL BONDING BETWEEN NORMAL CONCRETE SUBSTRATE AND ULTRA HIGH PERFORMANCE FIBER CONCRETE REPAIR MATERIAL

ABSTRACT

As a rule of thumb, the interfacial bonding between old concrete structures with a newly overlay repair material is one of the most important factors for structural functionality and safety as well as durability performance. In order to acquire an enhanced resistance against penetration of harmful substances, a good and effective bonding is necessary at the concrete interfaces. The objective of this study was to examine experimentally the mechanical properties and permeability characteristics short term and long term of the interface performance between normal concrete (NC) substrate which represented old concrete structures and an overlay of ultra high performance fiber concrete (UHPFC) as a repair material. The mechanical interfacial bond characteristics were assessed using the slant shear, splitting tensile, pull-off and flexural tests to quantify the influence of the differently roughened substrate surfaces and to assess the effect of different substrate moisture conditions. On the other hand, the permeability characteristics were evaluated by means of the rapid chloride permeability, gas and water permeability and porosity tests. Five types of surface textures were used: as cast (AC) (without surface preparation), sand blasted (SB), wire brushed (WB), with drilled holes (DH), and with grooves (GR). The roughness of the substrate surfaces was quantified using an optical three-dimensional surface metrology device (Alicona Infinite Focus). The microstructure of the interfacial transition zone was also studied using scanning electron microscopy and energy dispersive X-ray spectroscopy (SEM/EDS). The short and long term results showed that the newly overlay UHPFC achieved high bond strength and

bonds efficiently with the NC substrates. The pull-off test and flexural test results revealed that all failures occurred in the substrate, regardless of the substrate surface roughness. Majority of failures in the splitting tensile and slant shear test also occurred in the substrate. The composite UHPFC / NC substrate having a sand blasted surface behaved closely as a monolithic structure under splitting and slant shear tests. A very good correlation, mostly $R^2 > 80\%$ was obtained between the substrate roughness parameters and the results of the splitting cylinder tensile and slant shear tests. The permeability tests proved that the interfacial bonding was very good and efficient which significantly improved the impermeability of the composites. SEM/EDS proved that the use of UHPFC as repair material chemically, physically, and mechanically improved the repaired interfacial transition zone to become stronger and denser, as well as more uniform, and durable.

CHAPTER 1

INTRODUCTION

1.1 Background and Rationale

In this modern era, a highly developed infrastructure is vital for economic growth and prosperity of mankind. In many nations throughout the world, a lot of structures that constitute the whole infrastructure, especially those made of reinforced concrete, have suffered degradation which for some cases commenced after construction due to the combined effects of aggressive environments such as freeze-thaw cycles, deicing salts, marine exposure and significantly increasing live loads. Hence, some of the most important challenges faced by today's civil engineers are to save, retrofit and maintain these deteriorated structures. Implementation and development of new, efficient as well cost-effective rehabilitation and repair methods are required to extend the useful service life of the deteriorated structures (Green *et al.*, 2000).

The repair and rehabilitation of concrete structures have gained increasing market value over the past few years. For example, in United States the maintenance costs of bridges exceed 1 billion USD per year. The total maintenance costs of all types of structures can be assumed to exceed 20 billion USD per year. A significant part of these costs are spent on the repair and protection of concrete structures. Although the amount of work spent on building new structures has increased, works

related to repair and protection of these structures have also increased over time. The extensive development of new methods and materials for the repair and protection of concrete structures has led to the need for standards in such works and products (Raupach, 2006).

Repair and rehabilitation have recently drawn significant attention in the field of civil engineering. Although engineers have been repairing deteriorated structures for many years now, the rate of unsuccessful concrete repairs remains unacceptably high. Lack of knowledge on the influence of certain fundamental parameters is the reason of achieving durable repairs (Perez *et al.*, 2009a).

The early and premature deterioration of reinforced concrete structures is a serious issue for many nations, as it could put the public safety in jeopardy and the escalating repair cost could directly burden the future economy. In order to reduce this problem to a minimum and at the same time to maintain the basic functionalities and structural adequacies of these reinforced concrete structures, the frequency and extent of repair interventions should be kept to the lowest probable level (Denarié & Brühwiler, 2006).

As a rule of thumb, the interfacial bonding between deteriorated concrete structures with a newly overlay repair material is one of the most important factors for structural functionality and safety as well as durability performance. In order to

acquire an enhanced resistance against penetration of harmful substances, a good and effective bonding is necessary at the concrete interfaces.

1.2 Problem Statement

In the field of rehabilitation and strengthening of concrete structures, the need often arises to put new concrete next to old concrete. Examples of these applications are highway structures, where concrete overlays are used for rehabilitation of damaged concrete structures, and the deteriorated concrete must be replaced with new concrete. In these cases, the bond strength between the new and old concrete generally presents a weak link in the repaired structures. This is related to interfacial transition zone between new and old concrete is the weakest section in repaired concrete. Good adhesion and bonding at the interfaces in rehabilitated concrete structures is important for safety, durability, and better resistance against penetration of harmful substances (Gorst & Clark, 2003; Santos & Julio, 2011; Kuebitz, 2012).

Increasing the efficiency of the interfacial transition zone between the new and old concrete in terms of bond strength remains a challenge in concrete repair technology and is thus given considerable attention by researchers. This subject has been investigated numerous times, but only the bond strength as a value is addressed in most cases. The quantification of substrate surface roughness should be studied to better understand the bond mechanisms. Very few researches have studied the

permeability properties of the interfacial transition zone between the old and new concretes.

While more and more repair materials such as low slump dense concrete, high flow concrete, resin based repair mortar and concrete as well as polymer modified mortar and concrete have been developed in the market for concrete repair application using different techniques such as patching, overlaying, spraying as well as pressure grouting, the current concrete repair experiences portray a mixed bag of repair performance (Emmons, 1994; Russell, 2004). A large number of existing concrete structures worldwide are in urgent need for effective and durable repair. However, up to half of all concrete repairs are estimated to fail (Mather & Warner, 2003).

Ultra high performance fiber concrete (UHPFC) is one of the breakthroughs in concrete technology, providing significant improvement in strength, workability, ductility, and durability compared with normal concrete. The properties of UHPFC are enhanced through the reduction of the amount of water, removal of all coarse aggregates, use of highly refined silica fume, and introduction of steel fibers (Graybeal, 2007b). The improved durability and high compressive strength of ultra-high-performance fiber-reinforced concrete (UHPFC) suggest its potential as a conventional overlay material and solution; however, this application can only be ensured by a strong mechanical bond between the UHPFC as an overlay material and normal concrete (NC) as substrate material (El-Dieb, 2009).

Concrete repairs are often perceived to lack both early age performance and long-term durability. Approximately 75% of the failures can be attributed to the lack of durability. This inadequate performance is often ascribed to the lack of a reliable and perfect bond (Vaysburd & Emmons, 2000; Naderi, 2008). Therefore, it is of great research significance and challenge to develop effective and durable repair systems, which not only addressing the underlying concrete deterioration problems but also protecting the repaired concrete structures from the aggressive environment in the long run (Li & Li, 2006).

The research on the applications of UHPFC as a new material in construction is still in progress. Most of previous researches (Chui-Te Chiu & Wang, 2005) studied the properties of UHPFC as a new concrete material. Whereas researchers such as (Habel *et al.*, 2007) studied the used UHPFC as a composite material. There is serious dearth of information available about the behavior of UHPFC as a repair material. In addition, no research has been conducted to assess the bonding behavior of UHPFC as a repair material.

In this regard, this research aims at studying the early and the long term bonding behavior between UHPFC as a repair material and NC substrate as an old concrete. In case of the NC substrate, it was treated by different techniques, and the roughness parameters were quantified using an optical 3D surface metrology device (Alicona Infinite Focus). Different mechanical and permeability tests were also

utilized to assess the behavior of interfacial transition zone between UHPFC and NC substrate.

Moreover, the relationship between permeability tests and surface roughness are also studied, which has not yet been accomplished by any previous work in this field. None of the earlier studies investigated the permeability of the interfacial zone between substrate and repair. In general, mostly they focused on the mechanical properties of the interfacial zone.

1.3 Research Objectives

This research was carried out and designed based on four main objectives. The detailed objectives are as follows:

1. To investigate the bond strength characteristics between NC substrate and UHPFC as a repair material.
2. To examine the short and long term transport properties of the interfacial bond between NC substrate and UHPFC.
3. To quantify the influence of surface roughness of NC substrate on the interfacial bond characteristics of composite UHPFC/NC substrate.
4. To assess the influence of substrate surface moisture condition on the interfacial bond characteristics of composite UHPFC/NC substrate.

1.4 Scope

Two types of concrete were used in this study. The first type was normal concrete (NC) substrate which was used as an old concrete representing concrete from existing structure. The second type was the Ultra high performance fiber concrete (UHPFC) which was used as a repair material. Ordinary Portland cement (OPC) was used in both types of concrete. The mix proportions of the NC substrate and UHPFC were performed through a series of trial mixes to achieve a compressive strength of 45 MPa and 170 MPa at 28 days, respectively. Five types of NC substrate surface preparations were used in this study: (i) as-cast surface (AC); i.e. without surface preparation as reference; (ii) sand-blasted surface (SB); (iii) wire-brushed surface (WB); (iv) with drilled-holes surface (DH) and (v) with grooves surface (GR). Before casting the UHPFC onto the NC substrates, the roughened NC substrate specimens were divided into two categories according to the moistening methods, the first was 10 minutes moistening and wiped drying with a damp cloth, while the second was 24 hours moistening followed by 30 minutes drying. Steam curing was used to cure the UHPFC and the composite UHPFC/NC substrate. In this study no bonding agent was used between NC substrate and UHPFC. The experimental study involved in the determination of mechanical and permeability properties of NC substrate, UHPFC and the interface of the composite UHPFC/NC substrate specimens. Furthermore, the microstructure of the interfacial transition zone was studied using the scanning electron microscopy and energy dispersive X-ray spectroscopy (SEM/EDS).

1.5 Thesis outline

The present thesis comprises of five chapters. A brief layout of each chapter is given hereunder:

- Chapter one highlights the background of this work and also presents a short overview of related published works, problem statement, research objectives, as well as the scope of research.

- Chapter two reviews the literature on background of UHPFC definitions, properties, different applications in new constructions around the world and its suitability when used in repair and rehabilitation of old concrete structures. In addition, the different test methods for assessing bond strength are presented. Also the effect of roughness and moistening of the concrete substrate surface on the bond strength are discussed.

- Chapter three represents details of experimental works. It covers the methodology used in this research in order to achieve the objectives of this study. This chapter describes the materials properties and the mix design used in NC substrate and UHPFC. It also describes the casting of NC substrate specimens and the different surface preparation methods to afford the different types of roughness. Moreover the procedures for carrying out the experimental investigation, test apparatus used

in the determination of mechanical and permeability properties of NC substrate, UHPFC and the interface of the composite UHPFC/ NC substrate are highlighted.

- Chapter four presents the experimental results of the mechanical and permeability properties of NC substrate, UHPFC and the interface of the composite UHPFC/ NC substrate. Discussion and analysis of the results in terms of surfaces roughness parameters and moisture content of NC substrate are presented. The short and long-terms behavior of the composites are also discussed. In addition to this, the results of the microstructure of the interfacial transition zone of the composite UHPFC/ NC are discussed in detail.
- Chapter five is the final chapter outlining the research findings from the current observations and offers some recommendations for future research.

CHAPTER 2

Literature Review

2.1 Introduction

This chapter reviews the relevant literature related to the topic of this study. Some of the important findings with respect to ultra high performance fiber concrete, its preparation, properties and applications for various construction projects are discussed in detail.

2.2 Ultra high performance fiber concrete (definitions, contents, properties and applications)

The demand for high strength concrete (HSC) is increasing day by day owing to the spectacular progress made in terms of mega projects and high-rise complexes that are being constructed all around the world. One important aspect of HSC is that its definition has continuously changed over time and is expected to mean something else in near future. The last 2 decades have seen tremendous progress in the field of concrete science and technology that it far exceeds the total progress that was made over the previous 150 years (Graybeal, 2010). In the recent years the research in improving the performance of cementitious composites has yielded a construction material that possess as ultra-high performing material properties comparable with that of steel. The progress made with high-performance cementitious composites over the

years have resulted in a very good optimized grain-binder matrix suitable for both granular structure and the cementitious/binder composition, which are nowadays commonly referred to as Ultra-High-Performance Fiber-Reinforced Cement Composites (UHPFC). They showcase exemplary mechanical properties in terms of compressive strength, elastic modulus, tensile strength, and elastic post-cracking bending strength. Moreover, they are highly durable having a dense microstructure resulting in less or no porosity, water and gas permeability. Furthermore, it possesses negligible water absorption with very low diffusion coefficient (Toledo Filho *et al.*, 2012).

Figure 2.1 shows the classification of Fiber-Reinforced Concrete (FRC) that exhibit strain-hardening under uniaxial tension force. UHPFC which is the last developed type of FRC, is characterized by a dense matrix and, consequently, very low permeability when compared with high performance fiber reinforced cement composites (HPFRCC) and with normal-strength concretes (Habel *et al.*, 2006b).

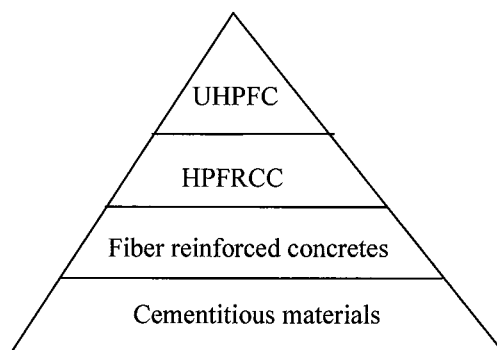


Figure 2.1: Classification of FRC.

2.2.1 Definition of Ultra high performance fiber concrete

UHPFC is an important type of construction material that was recently developed. This material has a very efficient high-technology cement-based matrix and high fiber content, which make it both extremely strong and very durable. However, this material is rarely used in real structures, due to the new design concepts that are required for its successful and cost-effective application (Morin *et al.*, 2001). It is an advanced cementitious material comprising a dense, high-strength matrix that contains a large number of evenly embedded steel fibers. UHPFC has exemplary mechanical and transport properties such as high tensile strength, strain hardening, and density that results in low permeability (Rossi, 2002).

When compared with HPC, UHPFC demonstrates better compressive behavior, tensile behavior, and durability (Parra-Montesinos *et al.*, 2005).

The significant improved properties of UHPFC is realized via the reducing in amount of mixing water, the removal of coarse aggregates, the use of highly refined silica fume and the introduction of steel fibers (Voort, 2008).

UHPFC are cementitious composites with outstanding material properties, it has very high strengths (compressive strength > 150 MPa, tensile strength > 8 MPa, flexural strength > 18 MPa) and display strain-hardening behavior under uniaxial tension. In addition the permeability of UHPFC is very low. (Voo *et al.*, 2011).

Ultra-high performance concrete (UHPC) is of the promising types of concrete that has been developed in the last decade. The efficiency of UHPC is particularly dependent on its density, which can be maximized by optimizing the particle packing to achieve ultra-high consolidation of the concrete matrix. The optimized particle packing can be achieved through an almost “perfect” grain size distribution by incorporating a homogeneous gradient of fine and coarse particles in the mixture (Ghafari *et al.*, 2012).

2.2.2 Ultra-high performance fiber concrete components

2.2.2.1 Typical Mix of Ultra high performance fiber concrete

The excellent properties of UHPFC are mainly achieved by improving the homogeneity of the mix compared with NC and by eliminating coarse aggregates. The grain size distributions of cement, silica fumes, and sand have to be optimized to achieve high capacity and, thus, a dense matrix with a very low permeability (Richard & Cheyrezy, 1995). Very finely graded sand with a size ranging from 150 μm to 600 μm is dimensionally the largest granular material in the mix. The second largest particle is cement, with an average diameter of 15 μm . Silica fume is the smallest particle used in the UHPFC. The main function of silica fume particles is to fill the interstitial voids between the cement and crushed quartz particles. Another fine particle is crushed quartz, which has an average diameter of 10 μm . Steel fibers are

dimensionally the largest components in the mix and are used to improve the ductility of the mix (Graybeal, 2005). Table 2.1 shows the ranges of UHPFC mix components.

Table 2.1: Range of UHPFC mix components (Graybeal, 2005).

Component	Typical range by weight (kg/m ³)
Sand	490 – 1390
Cement	610 – 1080
Silica Fume	50 – 334
Crushed Quartz	0 – 410
Fibers	40 – 250
Superplasticizer	9 – 71
Water	126 – 261

The following sections present a more detailed description of the role of each component of the UHPFC mix.

2.2.2.2 Ultra-high performance fiber concrete constituents

a. Sand

Sand serves as UHPFC aggregate. The elimination of coarse aggregates aids in improving the durability of UHPFC. Quartz sand is proposed for its high hardness and good paste–aggregate interfaces. The mean particle size is often smaller than 1 mm. However, UHPFC with maximum particle sizes of 8 mm to 16 mm has also been produced (Richard & Cheyrezy, 1995). Sand confines the cement matrix to add strength. In addition, variety of quartz sand that is not chemically active in the cement hydration reaction at room temperature is typically used (Porteneuve *et al.*, 2001).

b. Cement

Ordinary Portland Cement (OPC) is the primary binder used in UHPFC. The cement content ($\geq 700 \text{ kg/m}^3$) is more than two times higher than that for normal-strength concrete. The cement should have low alkali content, low to medium fineness, and low C_3A -content to reduce water requirements, ettringite formation, and heat of hydration. In most cases, CEM I 52.5 is used. However, promising alternatives such as CEM III/B are also available (Richard & Cheyrezy, 1995).

Interestingly, not all of the cement in the UHPFC matrix becomes hydrated because of the low water content of the mix. Although hydrated cement acts as a bonding agent,

unhydrated cement grains can act as high elastic modulus reinforcements in the matrix (Vernet, 2004).

c. Crushed Quartz

Given that not all of the cement is hydrated, a portion of unhydrated cement can be replaced by crushed quartz powder. Experimental works by Ma & Schneider (2002) showed that up to 30% of the volume of cement can be replaced by crushed quartz with no reduction in compressive strength. Aside from reducing the cement requirement, crushed quartz also improves the flowability of UHPFC mix.

d. Silica Fume

Silica fume, a highly reactive pozzolanic material, is a necessary ingredient for HPC and UHPFC. Silica fume was initially employed as early as 1969 in Norway; however its systematic application came to light in the early 1980s in North America and Europe. Since then, its demand has increased considerably either as partial replacement for cement or used as additive for special purpose cements, attributed to its desirable effects on the mechanical properties of cementitious composites (Mazloom *et al.*, 2004).

Silica fume is the smallest component in UHPFC with a diameter of 0.2 μm . It serves three basic functions in UHPFC:

- i. it fills voids between cement grains,
- ii. enhances the rheological characteristics, and forms hydration products by pozzolanic activity. The pozzolanic reaction refers to the reaction of silica hydrates with $\text{Ca}(\text{OH})_2$ (portlandite) produced by the hydration of OPC. The portlandite is consumed to produce C-S-H hydrates (Detwiler & Mehta, 1989; Goldman & Bentur, 1993; Megat Johari *et al.*, 2011).
- iii. in addition to this, silica fume content increases the length of C-S-H chains (Porteneuve *et al.*, 2001). Moreover, the mechanical strength is increased, and the microstructure and compacity of the UHPFC are also enhanced (Ma & Schneider, 2002).

e. Fibers

Although the UHPFC without fibers (Figure 2.2) demonstrates higher strength, it is also very brittle. The addition of fibers improves the ductility and increases its tensile properties. Moreover, the inclusion of steel fibers limits crack width and permeability by overcoming the propagation of microcracks and macrocracks that usually sets in normal concretes (Graybeal, 2005). Fibers carry tension forces across micro-cracks in the UHPFC. The orientation of fibers relative to the plane of cracking affects the ductile behavior of UHPFC. Thus, care must be taken in mixing and

placing UHPFC to avoid the clustering of fibers and to ensure proper fiber dispersion within each UHPFC element (Bayard & Ple, 2003).

The workability of any concrete mix that contains fibers is a function of both the fiber size and the coarse aggregate size in the mix. Given that UHPFC typically does not contain coarse aggregates, the dimensions of the fibers primarily affect concrete flowability. The workability of UHPFC mixes clearly decreases with increasing fiber size (Voo & Foster, 2010). A 2% fiber volume represents the most common content for UHPFC and corresponds with the most economic content identified by (Richard & Cheyrezy, 1995).

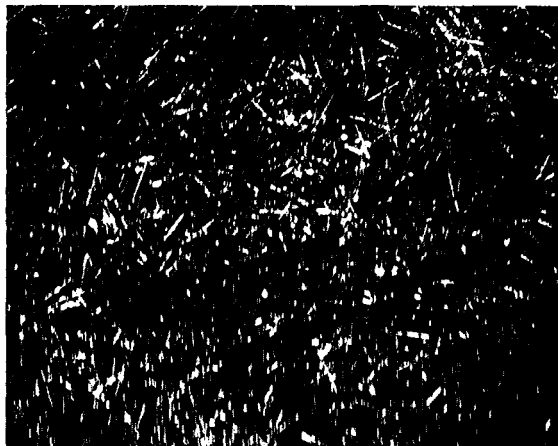


Figure 2.2: Steel fiber.

f. Superplasticizer

Superplasticizers are high-range water reducers made up of organic polymers. They are used to disperse cement particles and silica fume, and thus improves the flowability of UHPFC mixes. Thus, superplasticizers facilitate the achievement of a

lower water/cement (w/c) ratio and lower water/binder (w/b) ratio (binder includes both silica fume and cement) without sacrificing the workability of the mix. Given that UHPFC uses low w/c and w/b ratios, the optimum amount of superplasticizer is relatively high, with a solid content that is approximately 1.6% of the cement content (Richard & Cheyrezy, 1995). Superplasticizers of the third-generation polycarboxylates and polycarboxylate ethers are generally used for their high efficiency and lack of appropriate threshold for low w/c ratios (Habel, 2004).

g. Water

The goal in a UHPFC mix is not to minimize water content, but to maximize relative density (Schmidt *et al.*, 2003). The minimum w/b ratio for a workable mixture is 0.08 (Richard & Cheyrezy, 1995). The relative density, however, is not maximized at this w/b ratio, as shown in Figure 2.3. As the w/b ratio is increased above the 0.08 minimum, water replaces air without increasing the volume of the mixture up to a w/b ratio of approximately 0.13. In case the w/b ratio is increased beyond 0.13, the volume increases on account of additional water and as a consequence density of the mixture decreases significantly. In Figure 2.3, the mixtures represented by the descending branch of the graph have superior performance and workability compared with those represented by the ascending branch. Thus, the practical optimum w/b ratio used is chosen to be slightly toward the higher values of the w/b ratio to ensure that the w/b ratio of the actual mixture is slightly higher than the theoretical optimum (Voort, 2008).

Richard and Cheyrezy (1995) identified 0.14 as the optimal w/b ratio for UHPFC, which agrees exactly with the study by De Larrard & Sedran (1994) where a solid suspension model was used. The result also agrees closely with that of Gao et al., (2005), where an optimum w/b ratio of 0.15 was reported based on experimental test samples.

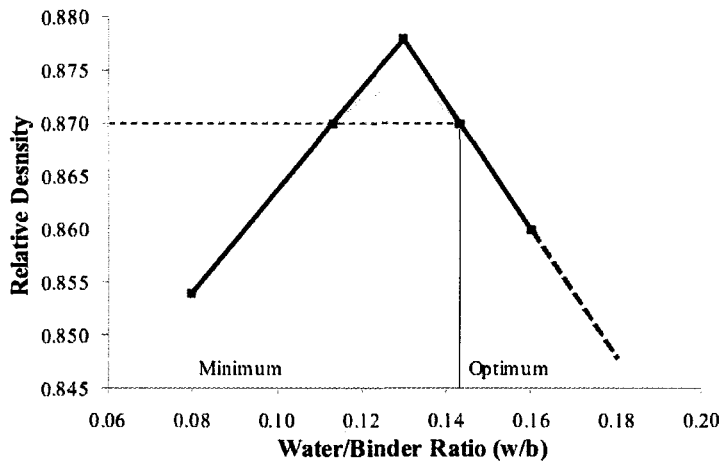


Figure 2.3: Relative density versus water content (Richard and Cheyrezy, 1995)

2.2.3 Properties of Ultra-high performance fiber concrete

2.2.3.1 Tensile behavior

One of the concrete types belonging to the HPFRCC group is the UHPFC. In addition to its regular high performing features it has additional advantage of being a very dense low-permeable matrix. A comparative study of the uniaxial tensile behavior for UHPFC, conventional steel fiber-RC (SFRC), and conventional concrete are depicted in Figure 2.4. The results clearly show that UHPFC exhibits higher tensile strength and strain-hardening behavior when compared to other cementitious materials (Habel, 2004).

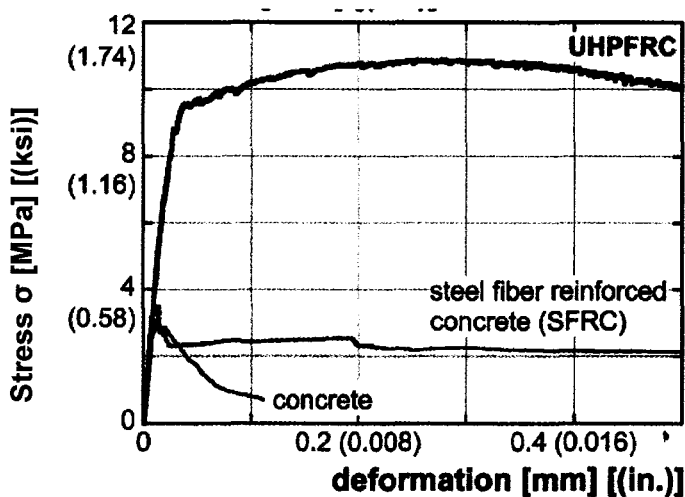


Figure 02.4: Uniaxial tensile behavior: comparing UHPFC, conventional SFRC, and conventional concrete (Habel, 2004).

2.2.3.2 Flexural Strength

UHPFC showcases very high flexural strength and extremely good ductility behavior about 250 times greater conventional concrete (Voo & Foster, 2010). The behavior of UHPFC under flexure loading can be characterized by three phases:

- I. the linear elastic behavior up to the first cracking strength of the material,
- II. a displacement-hardening phase up to the maximum load, and
- III. a deflection-softening phase after the maximum load is reached.

Figure 2.5 shows the load-deflection diagram for UHPFC during bending with the typical phases labeled (Acker & Behloul, 2004b).

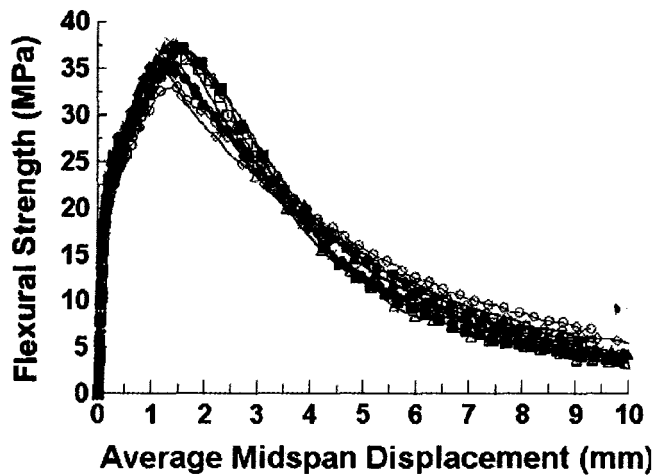


Figure 2.5: Flexural strength versus midspan displacement (Voo & Foster, 2010)

2.2.3.3 Durability

The greatly improved microstructure of UHPFC not only results in higher compressive strength but also leads to greater durability. These properties make UHPFC both a high-strength and high-performance material. The very low porosity of UHPFC, particularly capillary porosity, greatly improves its durability (Voort, 2008). The various durability properties for UHPC compared with HPC and NC are compiled in Figure 2.6 (Voort, 2008). The exceptional durability property of UHPC reduces the maintenance costs and possibly decreases the cover concrete required to resist weathering effects compared with NC.

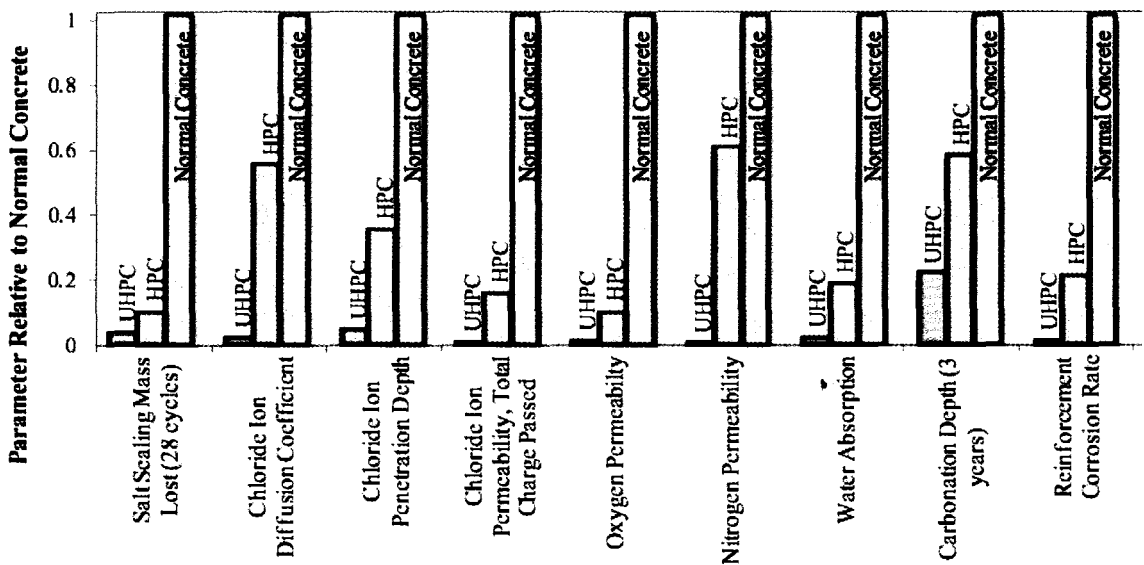


Figure 2.6: Durability of UHPC and HPC versus NC (lowest values identify the most favorable material) (Voort, 2008)

2.2.3.4 Curing of UHPFC

In order to avail all the superior benefits arising from UHPFC, steam curing treatment must be utilized. Several researchers have reported that the standard heat curing after the initial curing lasts for 48 h at 90 °C, as shown in Figure 2.7. (Ujike *et al.*, 2006), (Wu *et al.*, 2009), (Farhat *et al.*, 2010), (Voo & Foster, 2010), (Graybeal, 2011), (Trinh & Chanh, 2012).

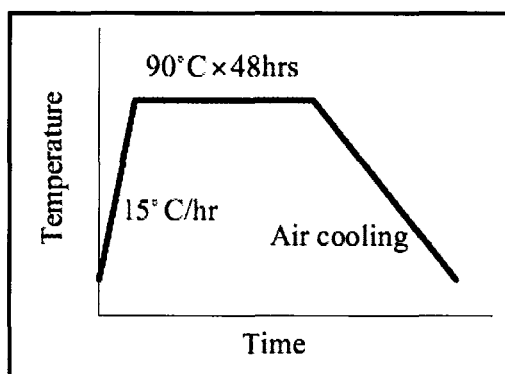


Figure 2.7: Conditions of standard heat curing (Ujike *et al.*, 2006)

Heat curing promotes high density and high strength, reduces delayed shrinkage and creep effects, and improves durability (Richard & Cheyrezy, 1995). Moreover, it must be accomplished only after the concrete has set to avoid any risk of delayed ettringite formation and therefore it requires good knowledge of setting time (Resplendino & Petitjean, 2003).

The total porosity of UHPC appears to depend on the curing process applied to the material. Figure 2.8 shows the cumulative porosity of both a heat-treated and an